A Generic Approach to Desired Metallic Nanowires Inside Native Porous Alumina Template via Redox Reaction

Qiaoling Xu, Guowen Meng,* Xuebang Wu, Qing Wei, Mingguang Kong, Xiaoguang Zhu, and Zhaoqin Chu

Key Laboratory of Materials Physics and Anhui Key Laboratory of Nanomaterials and Nanostructures, Institute of Solid State Physics, Chinese Academy of Sciences, Hefei 230031, People's Republic of China

Received December 22, 2008. Revised Manuscript Received February 27, 2009

We report a facile, economic, and generic way to mono- and multisegment metallic nanowires (MNWs) of various pure metals (e.g., Au, Pt, Pd, Cu, Ni, and Co) and their alloys with both linear and branched topologies, by merely infiltrating aqueous solutions of metal chloride salts into Au-coated native porous anodic aluminum oxide template with Al foil on its outside edge. Redox reactions of two galvanic cells where the Al foil acts as the anode are responsible for the formation of the MNWs. Redox reaction of the top galvanic cells on the surrounding Al foil leads to the formation of metal atoms on the Al foil surface, which subsequently diffuse away from the Al foil and into the nanochannels. Simultaneously, redox reaction of the bottom galvanic cell where the Au layer serves as a cathode results in the formation of metal atoms on the top surface of the bottom Au layer, followed by crystal nucleus formation and growth upward the channels to form short MNWs. With the elongation of the infiltration duration, the diffusing metal atoms coming from the top galvanic cells reach the tips of the growing MNWs, and combine with those on the MNW tips coming from the bottom galvanic cell, resulting in longer MNWs under the nanochannel geometrical confinement. The approach enables excellent control over the composition, location, length, and diameter of the individual segments and the topology of the overall NWs that are promising for many applications in nanotechnology.

Introduction

Metallic nanowires (MNWs) have been the focus of intensive research because of their attractive electrical, optical, magnetic, and thermal properties, with potential applications in microelectronics, optoelectronics, magnetic manipulation, biotechnology, catalysis, and sensors.[1−10] Tremendous efforts have been devoted to the synthetic approaches of the MNWs, mainly including porous-template-assisted synthesis[3,8−20] and capping-agent-controlled crystal growth.[5,21,22] Comparatively, porous-template-assisted electrodeposition[11−15] and electroless deposition[16−20] are the most popular techniques. However, for the porous-template-assisted electrodeposition, electric power is required, whereas for the conventional porous-template-assisted electroless deposition, metallic ions are typically reduced in the presence of organic surfactants,[17,20] and pore walls of the template are usually modified via a complex sensitization−preactivation process.[16−19] Here, neither electric power nor organic surfactants, nor modifying on the pore walls is required, by simply infiltrating aqueous solutions of metal chloride salts into native porous anodic aluminum oxide (AAO) template with ring-shaped Al foil surrounded on its circumjacent outside edge and an Au layer coated on the bottom surface side (ab. Au-coated, Al-surrounded AAO template), we

* To whom correspondence should be addressed. E-mail: gwmeng@issp.ac.cn.

(1) Pascual, J. I.; Mendez, J.; Gomez-Herrero, J.; Baro, A. M.; Garcia, N.; Landman, U.; Luedtke, W. D.; Bogachek, E. N.; Cheng, H. P. *Science* **1995**, *267*, 1793–1795.
(2) Cui, Y.; Wei, Q.; Park, H.; Lieber, C. M. *Science* **2001**, *293*, 1289–1292.
(3) Cai, L. T.; Skulason, H.; Kushmerick, J. G.; Pollack, S. K.; Naciri, J.; Shashidhar, R.; Allara, D. L.; Mallouk, T. E.; Mayer, T. S. *J. Phys. Chem. B* **2004**, *108*, 2827–2832.
(4) Yun, M.; Myung, N. V.; Vasquez, R. P.; Lee, C.; Menke, E.; Penner, R. M. *Nano Lett.* **2004**, *4*, 419–422.
(5) Murphy, C. J.; Gole, A. M.; Hunyadi, S. E.; Orendorff, C. J. *Inorg. Chem.* **2006**, *45*, 7544–7554.
(6) Weeber, J.; Dereux, A.; Girarad, C.; Krenn, J. R.; Goudonnet, J. *Phys. Rev. B* **1999**, *60*, 9061–9068.
(7) Barnes, W. L.; Dereux, A.; Ebbesed, T. W. *Nature (London)* **2003**, *424*, 824–830.
(8) Liu, F.; Lee, J. Y.; Zhou, W. J. *Small* **2006**, *2*, 121–128.
(9) Dickson, R. M.; Lyon, L. A. *J. Phys. Chem. B* **2000**, *104*, 6095–6098.
(10) Reich, D. H.; Tanase, M.; Hultgren, A.; Bauer, L. A.; Chen, C. S.; Meyer, G. J. *J. Appl. Phys.* **2003**, *93*, 7275–7280.
(11) Liu, J.; Duan, J. L.; Toimil-Molares, M. E.; Karim, S.; Cornelius, T. W.; Dobrev, D.; Yao, H. J.; Sun, Y. M.; Hou, M. D.; Mo, D.; Wang, Z. G.; Neumann, R. *Nanotechnology* **2006**, *17*, 1922–1926.
(12) Kim, W. J.; Carr, S. M.; Wybourne, M. N. *Appl. Phys. Lett.* **2005**, *87*, 173112.
(13) Schönenberger, C.; van der Zande, B. M. I.; Fokkink, L. G. J.; Henny, M.; Schmid, C.; Kru1ger, M.; Bachtold, A.; Huber, R.; Birk, H.; Staufer, U. *J. Phys. Chem. B* **1997**, *101*, 5497–5505.
(14) Sehayek, T.; Vaskevich, A.; Rubinstein, I. *J. Am. Chem. Soc.* **2003**, *125*, 4718–4719.
(15) Nielsch, K.; Müller, F.; Li, A.-P.; Gösele, U. *Adv. Mater.* **2000**, *12*, 582–586.
(16) Menon, V. P.; Martin, C. R. *Anal. Chem.* **1995**, *67*, 1920–1928.
(17) De Leo, M.; Pereira, F. C.; Moretto, L. M.; Scopece, P.; Polizzi, S.; Ugo, P. *Chem. Mater.* **2007**, *19*, 5955–5964.
(18) Yang, C.-M.; Sheu, H.-S.; Chao, K.-J. *Adv. Funct. Mater.* **2002**, *12*, 143–148.
(19) Yuan, X. Y.; Wu, G. S.; Xie, T.; Lin, Y.; Zhang, L. D. *Nanotechnology* **2004**, *15*, 59–61.
(20) Wirtz, M.; Martin, C. R. *Adv. Mater.* **2003**, *15*, 455–458.
(21) Kim, J.-U.; Cha, S.-H.; Shin, K.; Jho, J. Y.; Lee, J.-C. *Adv. Mater.* **2004**, *16*, 459–464.
(22) Lee, E. P.; Chen, J.; Yin, Y.; Campbell, C. T.; Xia, Y. *Adv. Mater.* **2006**, *18*, 3271–3274.

10.1021/cm803458b CCC: $40.75 © 2009 American Chemical Society
Published on Web 03/27/2009

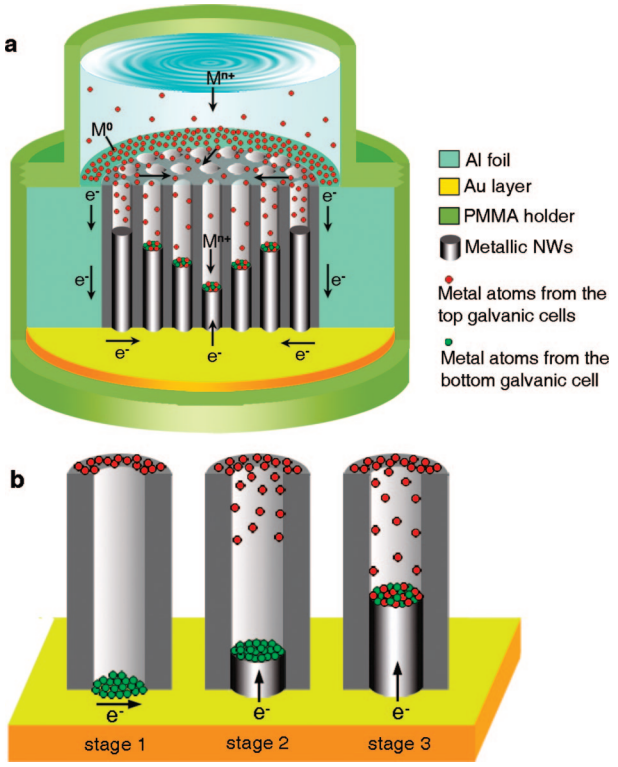

Figure 1. Schematic for the formation of the MNWs inside the vertically aligned nanochannels of the Au-coated, Al-surrounded AAO template. (a) The simple setup for the formation of the MNWs. (b) The detailed formation process of the MNWs, with three different representative stages: stage 1, metal atom formation on both the Al foil top surface and the bottom Au layer; stage 2, crystal nucleus formation and NW growth from metal atoms coming from the bottom galvanic cell; and stage 3, NW growth from metal atoms coming from both the top and bottom galvanic cells.

report a generic synthetic approach to mono- and multisegment MNWs of various pure metals (e.g., Au, Pt, Pd, Cu, Ni, and Co) and their alloys with both linear and branched morphologies. The formation of the MNWs is attributed to redox reactions of two galvanic cells to form metal atoms and subsequent nanochannel-confined growth. The obtained MNWs with tunable composition and morphologies have potentials in nanodevices and nanosystems.

Experimental Section

Preparation of the MNWs. The Al-surrounded AAO templates were prepared via a two-step anodization process.[23] The ring-shaped surrounding Al foil was achieved by protecting a circumjacent part of the Al foil from the electrolyte during the whole fabrication process of the AAO template (see Figure S1 in the Supporting Information). An Au layer (100 nm) was sputtered onto one planar surface side of the Al-surrounded AAO template with two-end-through pores. Aqueous solution of metal chloride salts (2 mL) was infiltrated into the Au-coated, Al-surrounded AAO template mounted in a simple polymethyl methacrylate (PMMA) holder (Figure 1a). The whole infiltration was performed at 25 °C. After infiltration, the template, together with the resultant products, was taken out from the holder, rinsed with deionized water, and dried at room temperature. The AAO template embedded with the resultant products exhibits an intense dark color, being much different from its initial golden color (see Figure S2 in the Supporting Information). For MNWs of elemental Au, Pt, Pd, Cu, Ni, and Co, aqueous solutions of their corresponding water-soluble salts of $HAuCl_4 \cdot 4H_2O$, $H_2PtCl_6 \cdot 6H_2O$, $(NH_4)_2PdCl_4$, $CuCl_2 \cdot 2H_2O$, $NiCl_2 \cdot 6H_2O$, and $CoCl_2 \cdot 6H_2O$ were used, respectively. Compound NWs of metal alloy AuPt were obtained by using a mixed aqueous solution of $HAuCl_4 \cdot 4H_2O$ and $H_2PtCl_6 \cdot 6H_2O$. Two-segment NWs of Au and Ni were achieved by sequentially infiltrating aqueous solutions of $HAuCl_4 \cdot 4H_2O$ and $NiCl_2 \cdot 6H_2O$ into the same piece of Au-coated, Al-surrounded AAO template. Three-segment NWs of Au−Ni−Au were synthesized via sequential infiltration with aqueous solutions of $HAuCl_4 \cdot 4H_2O$, $NiCl_2 \cdot 6H_2O$, and $HAuCl_4 \cdot 4H_2O$. It should be noted that before infiltrating the metal chloride aqueous solutions, insulating adhesive tapes were stuck on most surface of the Al foil and only leave a very narrow ring-shaped part exposed.

Characterization of the MNWs. The morphology and structure of the MNWs were characterized by using X-ray diffraction (XRD, X' Pert Pro MPD), scanning electron microscopy (SEM, SIRION 200), transmission electron microscopy (TEM), high-resolution TEM, and selected area electron diffraction (HRTEM/SAED, JEM-2010). For SEM and TEM observations, the MNWs were released by dissolving the AAO templates in a 3 M NaOH aqueous solution, and then washed repeatedly with deionized water.

Results and Discussion

As chloride ions can break down the surface alumina layer on pure Al foil,[24] and pure Al has a lower redox potential [Al^{3+}/Al, −1.67 V vs SHE (standard hydrogen electrode)][25] than that of a large variety of metallic ions, here we have developed a simple, economic, and generic method for fabricating MNWs by infiltrating aqueous solutions of metal chloride salts into the Au-coated, Al-surrounded AAO template, based on redox reactions of two galvanic cells to form metal atoms and subsequent nanochannel-confined growth. Figure 1 schematically shows the formation of the MNWs inside the nanochannels of the Au-coated, Al-surrounded AAO template. When metal chloride aqueous solution is filled in the simple setup and reaches the surrounding Al foil on the outside region, chloride ions in the solution will etch away the dull alumina layer on the pure Al foil and pure Al is exposed. Redox reactions of two galvanic cells in which the exposed Al foil serves as an anode lead to simultaneous formation of zero-valence metal atoms (M^0) on both top surface of the surrounding Al foil and the bottom Au layer at the initial stage of the infiltration process as follows: (i) The lower redox potential of Al (Al^{3+}/Al) than that of a large variety of metallic ions (M^{n+}/M) enables the spontaneous electron transfer from the Al foil (oxidation) to the metallic ions, leading to the reduction of the metallic ions into metal atoms on the top surface of the Al foil. In these galvanic cells, some locations on the Al foil surface serve as anodes, where Al is oxidized into Al^{3+} that subsequently enters into the solution

$$Al \rightarrow Al^{3+} + 3e^-$$

The electrons then transfer to the cathodes (some other locations on the Al foil surface) across the Al foil itself,

(23) Masuda, H.; Satoh, M. *Jpn. J. Appl. Phys* **1996**, *35*, L126–L129.

(24) Djokić, S. S. *J. EIectrochem. Soc.* **1996**, *143*, 1300–1305.

(25) Bard, A. J.; Parsons, R.; Jordan, J. *Standard Potentials in Aqueous Solution*; Marcel Dekker: New York, 1985.

where the metallic ions in the solution gain electrons and are reduced into metal atoms

$$M^{n+} + ne^- \rightarrow M^0$$

(ii) The formation of metal atoms on the bottom Au layer is accomplished via the redox reaction of a galvanic cell similar to that reported previously,[26] in which the Al foil acts as an anode where Al dissolution takes place, whereas the Au layer (in good electrical contact with the Al foil) serves as a cathode, where metal atom deposition occurs. The redox reactions on the electrodes are the same as those described in the previous part (i).

The detailed formation process of the MNWs in the nanochannels is illustrated in Figure 1b. At the initial stage of the infiltration process, metal atoms are formed simultaneously on both the Al foil via redox reactions of the top galvanic cells on the surrounding Al foil and the bottom Au layer via redox reaction of the bottom galvanic cell where the Al foil acts as an anode and the Au layer serves as a cathode (stage 1). When metal atoms on the Al foil surface start to diffuse away from the Al foil and some will diffuse into the nanochannels because of the concentration gradient, those formed on the bottom Au layer nucleate and grow upward the channels from metal atoms continuously formed via redox reaction of the galvanic cell where the formed MNWs (together with bottom Au layer) serves as cathodes. In this galvanic cell, the electrons on the Al foil top surface transfer (through ring-shaped Al foil) down to the bottom, and then through the Au layer to the MNWs. Subsequently, metallic ions in the solution gain electrons on the tips of the MNWs and metal atoms are formed (stage 2). With the elongation of the infiltration duration, the diffusing metal atoms coming from the top galvanic cells will reach the tips of the MNWs, and combine with those on the MNW tips coming from the bottom galvanic cell, resulting in longer MNWs under the nanochannel geometrical confinement (stage 3). Theoretically, MNWs of any metals could be achieved if their corresponding water-soluble chloride salts are employed and their metallic ions have a higher redox potential than that of Al. Herein, we shall describe Au nanowires (NWs) achieved via simply infiltrating the Au-coated, Al-surrounded AAO template with aqueous solution of $HAuCl_4 \cdot 4H_2O$ ($AuCl_4^-$/Au, +1.002 V vs SHE);[25] one can easily extend this approach to MNWs of other metals (e.g., Pt, Pd, Cu, Ni, and Co).

After the template is infiltrated with $HAuCl_4$ aqueous solution and dried, XRD measurement (Figure 2a) confirms that the resultant products embedded in the AAO template are crystalline gold with face-centered cubic (fcc) lattice structure (JPCDS 04−0784). SEM observations (images b and c in Figure 2) show that large quantities of Au NWs, with all the wires having the same diameters and each wire having uniform diameter along its axis, have been achieved. It should be mentioned that the diameters of the Au NWs are about 55−60 nm, in agreement with the diameter of the nanochannels inside the template (prepared in $C_2H_2O_4$ electrolyte). Figure 2d is a TEM image of a typical single

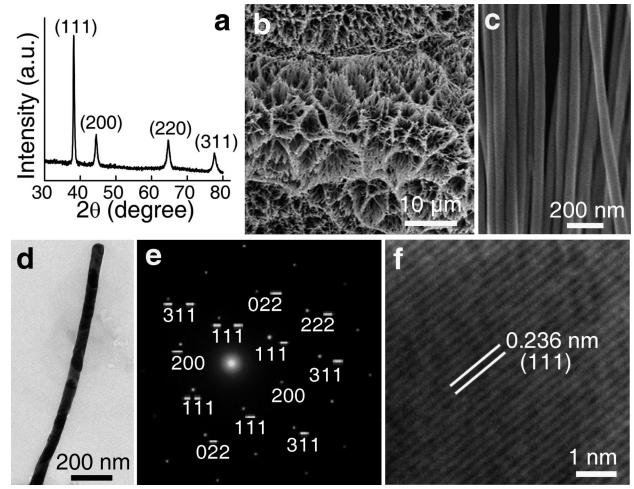

Figure 2. Au NWs achieved in a 10 mM $HAuCl_4$ aqueous solution with infiltration duration of 3 h. (a) XRD pattern taken from the NWs embedded in AAO template. (b) Low-magnification SEM image of the Au NWs (top-view) after template removal. (c) High-magnification SEM image of a bundle of the Au NWs (side-view). (d) TEM image of a single NW. (e) SAED pattern taken from the Au NW shown in (d). (f) HRTEM image of the same NW.

Au NW. SAED pattern taken from this NW (Figure 2e) can be ascribed to fcc single-crystal gold viewed along the [011] orientation, revealing that the Au NWs are single crystalline, which is further confirmed by lattice-resolved image (Figure 2f). We then carefully examined the lengths of the Au NWs located in three areas with different distances from the boundary of surrounding Al and AAO template (see Figure S3 in the Supporting Information). The results show that the closer the nanochannels are to the Al−AAO boundary, the longer the NWs formed in the corresponding channels would be. This could be ascribed to the shorter diffusion distance of the Au atoms coming from the surrounding Al foil, and local temperature increase of the solution near the Al foil, which is caused by redox reactions of the top galvanic cells, leading to faster diffusion of Au atoms into the nanochannels near the Al−AAO boundary.

The formation mechanism of the MNWs has been confirmed in the following. As for the Al reduction of metallic ions into metal atoms, we immersed a piece of Au-coated native AAO template without surrounding Al foil into $HAuCl_4$ aqueous solution for 1 h, there was no change in color (see Figure S4a in the Supporting Information), indicating that no Au products formed. However, when we immersed the same piece of Au-coated native AAO template into the same $HAuCl_4$ solution and then dropped a very small piece of Al foil in the solution, as expected, the Au-coated native AAO template became dark from golden (see Figure S4b in the Supporting Information), implying that Au products (atoms or NWs) were formed inside the nanochannels of the template. Therefore, the surrounding Al foil plays a key role in the reduction of $AuCl_4^-$ ions to Au atoms.

To further confirm the formation mechanism of the MNWs, we have carried out a similar infiltration process by using an Al-surrounded AAO template without bottom Au layer. After the template was infiltrated with $HAuCl_4$ aqueous solution, we found a small amount of Au NWs deposited in the nanochannels near the Al foil (see a and b in Figure S5

(26) Qu, L. T.; Dai, L. M. *J. Am. Chem. Soc.* **2005**, *127*, 10806–10807.

of the Supporting Information). Without the bottom Au layer, it is obvious that the only source for the Au atoms is from redox reactions of the top galvanic cells on the Al foil surface. These results provide a convincing evidence for the diffusion of the Au atoms into the nanochannels to form Au NWs. The diffusion of Au atoms in the solution can be ascribed to the atom concentration gradient. For pure diffusion in the solution, the flux of Au atoms is described with Fick's first law as follows

$$J = -D\frac{dC}{dx}$$

Where J is the flux of Au atoms, D is the diffusion coefficient of Au atoms, and dC/dx is the concentration gradient of Au atoms. After the infiltration of $HAuCl_4$ aqueous solution into either Au-coated, Al-surrounded AAO template or Al-surrounded AAO template without bottom Au layer, we can observe some golden products floating on the solution and some black products staying on the exposed Al foil when the area of the Al foil exposed in the solution is too large. These products were confirmed to be Au clusters by SEM and energy-dispersive spectroscopy (EDS) (see c and d in Figure S5 of the Supporting Information). This is attributed to the formation of large amount of Au atoms on the Al foil in a short time because of the large area of Al exposed to the solution. It should be mentioned that macroscopic clusters on the Al foil surface would prevent subsequent redox reactions. The solution to this problem is to leave only a very narrow ring-shaped part of the Al foil surface exposed in the solution. Under this condition, no macroscopic clusters are formed even if the diffusion of Au atoms is slow, because the occurrence of concentration polarization on the cathode will make the reduction of the metallic ions into metal atoms slow, resulting in a balance for total amount of Au atoms on the Al foil.

To investigate the detailed formation process of the MNWs, we purposely prepared one sample with very short infiltration duration. SEM observation reveals that very short Au nanorods (or even nanodots) are formed on the bottom Au layer (see Figure S6 in the Supporting Information), indicating that the formation of the NWs initiates at the bottom Au layer. This result provides evidence that some Au atoms are formed via redox reaction of the bottom galvanic cell, where the Au layer serves as a cathode. We then deliberately synthesized another three samples with the same $HAuCl_4$ concentration with longer infiltration durations. SEM observations of these Au NWs (from the three samples) at locations with similar distances from the Al−AAO boundary show that longer infiltration duration results in longer Au NWs (see Figure S7 in the Supporting Information), indicating that with the elongation of the infiltration duration, the NWs grow longer and longer under the nanochannel confinement.

Further experiments demonstrate that higher $HAuCl_4$ concentration also leads to longer Au NWs (see Figure S8 in the Supporting Information) under the same infiltration duration, which could be ascribed to more Au atoms achievable from higher $HAuCl_4$ concentration. In addition,

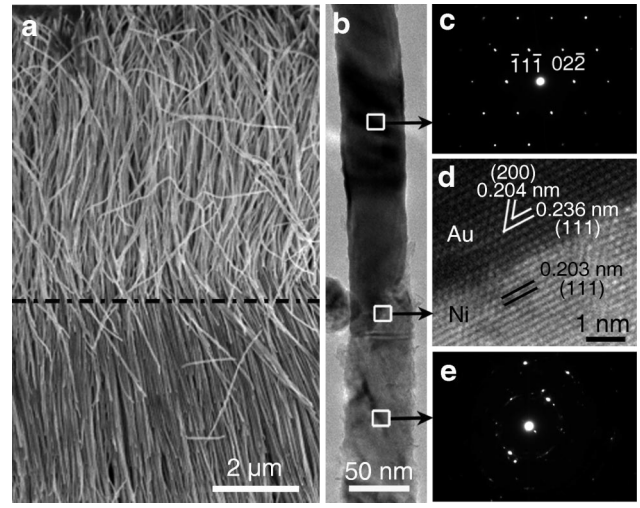

Figure 3. Two-segment MNWs consisting of nonmagnetic metal Au and magnetic metal Ni. The Ni segments were achieved in a 5 M $NiCl_2$ aqueous solution with infiltration duration of 20 min, whereas the Au segments were obtained by a subsequent infiltration in a 10 mM $HAuCl_4$ aqueous solution for 1 h. (a) Side-view SEM image, with a black dashed line showing the interface of the two segments having different contrasts. (b) TEM image near the junction area, along with the SAED patterns taken from (c) the Au segment and (e) the Ni segment, respectively, and (d) lattice-resolved image of the Au−Ni interface.

our experiments show that the diameters of the resultant Au NWs are in agreement with those of the nanochannels inside the templates used in the infiltration process (Figure 2c and Figure S9 in the Supporting Information, Au NWs achieved from the templates with different pore diameters prepared in $C_2H_2O_4$ and H_2SO_4 electrolyte, respectively), further demonstrating the nanochannel-confined growth of the MNWs. Therefore, Au NWs with desired length and diameter can be achieved by simply tuning the $HAuCl_4$ concentration, infiltration duration, and pore diameter of the template used.

On the basis of what we have demonstrated for Au NWs, other water-soluble metal chloride salts with their metallic ions having a higher redox potential than that of Al (see Table S1 in the Supporting Information) could also be used to achieve their corresponding MNWs by using our approach. For example, MNWs of element Pt, Pd, Cu, Ni, and Co have been already achieved (Figures S10−S14 in the Supporting Information). Moreover, compound NWs of metal alloys consisting of the above-mentioned metals could also be achieved if a mixed aqueous solution of the two desired metal chloride salts is utilized in the infiltration process (see Figure S15 in the Supporting Information, compound MNWs of metal alloy AuPt). Furthermore, segmented MNWs consisting of different metals or alloys with distinct properties could also be achieved by sequentially infiltrating the corresponding aqueous solutions of metal chloride salts into the same piece of Au-coated, Al-surrounded AAO template. Figure 3 shows two-segment MNWs consisting of nonmagnetic metal Au NW as one segment and magnetic metal Ni NW as its neighboring segment. SEM observation (Figure 3a) shows that the two segments have different contrasts, and EDS measurements reveal that the right compositions of the materials have been deposited in sequence (see Figure S16 in the Supporting Information). Figure 3b is a TEM image of the two-segment NW of Au and Ni, and SAED patterns

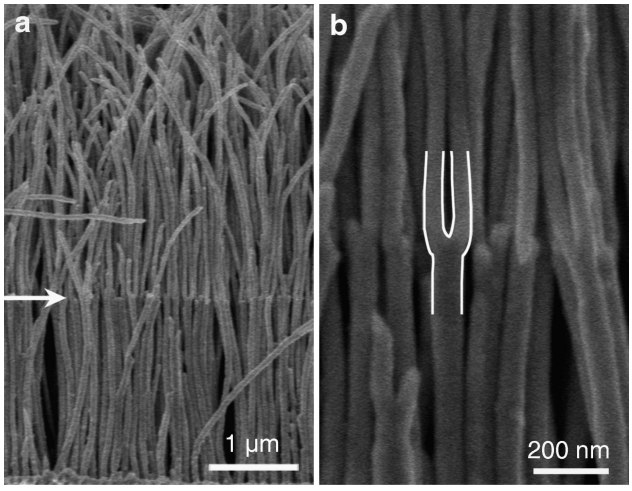

Figure 4. Y-branched Au NWs achieved in a 10 mM $HAuCl_4$ aqueous solution with infiltration duration of 2 h. (a) Low-magnification SEM image of a bundle of the Y-branched Au NWs after template removal, with a white arrow marked on the interface showing the locations where the Y-branchings take place. (b) High-magnification SEM image of the NWs near the Y-junction region with stems and branches about 80 and 50 nm in diameter, respectively. One of the Y-junction is contoured in white lines for clarity.

(c and e in Figure 3) taken from the two segments reveal that the dark contrast segment is single-crystalline Au NW, whereas the light contrast segment is polycrystalline Ni NW. Lattice-resolved image (Figure 3d), taken on the junction interface of Au and Ni segments, reveals that Au (111) plane is nearly parallel to Ni (111) plane. Similarly, multisegment MNWs with individual segments having distinct properties also could be achieved via multiple sequential infiltrations. For example, three-segment MNWs consisting of nonmagnetic metal Au NW, magnetic metal Ni NW, and nonmagnetic metal Au NW in sequence, have been achieved (see Figure S17 in the Supporting Information). Finally, our approach could not only be used for linear MNWs (as all those demonstrated above) but also be extended to produce MNWs with branched morphology or even more complex shapes (e.g., multiple generations of Y-branching and multiple branchings from one stem), if AAO template with the corresponding complex-shaped nanochannels is used.[27] As an example, we have demonstrated MNWs with the simplest branched morphology, i.e., Y-branched NWs of Au, as shown in Figure 4.

After our paper was published online (ASAP), it was said that a similar approach had already been used for the fabrication of Cu NWs.[28] We eagerly read the paper and found that the formation mechanism of Cu NWs in the reported paper is also based on redox reactions of the galvanic cell. However, our approach differs from the reported method and has some advantages as follows: (i) In the reported method, the Al foil is separated from the AAO templates and stuck on the Au layer by using a conductive paste; in our approach, the Al-surrounded AAO templates were achieved in our fabrication process of the AAO template. This special structure facilitates good electrical contact between the Al foil and Au layer and makes the experimental manipulation much easier and convenient. For our approach, we also found that metal atoms responsible for the formation of MNWs were formed not only on the Au layer but also on the surrounding Al foil surface. (ii) In the reported method, the whole template was immersed in the solution; in our approach, the solution was infiltrated into the Al-surrounded AAO templates from their top surfaces. This can avoid large-area contact between the Al foil and the solution. (iii) In the reported method, the solution used was mixed solution of copper sulfate and boric acid. Using such mixed solution, Cu NWs can be obtained with long reaction time (7 h to several days). Therefore, the reported method is suitable for the fabrication of Cu NWs; in our approach, the aqueous solution is merely containing metal chloride salt suitable for preparing a large variety of MNWs with short infiltration duration (tens of minutes to several hours). Therefore, our method is a generic approach. It should be mentioned further that because the chloride ions can break down the surface alumina layer on the Al foil,[24] the use of metal chloride salts facilitates redox reactions of the galvanic cells in our approach.

Conclusion

In summary, by merely infiltrating Au-coated, Al-surrounded AAO template with aqueous solutions of metal chloride salts, we have developed a facile, low-cost, and generic way to large-scale arrays of various MNWs, based on redox reactions of two galvanic cells to form metal atoms and subsequent nanochannel-confined growth. By simply selecting the desired water-soluble metal chloride salts, tailoring their aqueous solution concentrations, tuning the infiltration sequence and durations, and infiltrating the solutions into the nanochannels of the AAO template with desired channel diameter and morphology, we can achieve both linear and branched mono- and multisegment MNWs of various metals and their alloys, with each and every segment having desired chemical composition, location, length, and diameter. From the point of view of methodology, our approach to MNWs is generic (suitable for a large variety of metals). Compared with the most popularly used porous-template-assisted electrodeposition of MNWs,[11−15] the present method is energy saving (without using electric power); whereas compared with the conventional porous-template-assisted electroless deposition of MNWs,[16−20] our approach is facile (no modification with functional silanes, Ag, or Pd particles on the pores) and green (without using organic surfactants). Our simple, economic, and generic approach paves the way for the future nanotechnology where large quantities of predesigned MNWs are required.

Acknowledgment. We thank the National Science Fund for Distinguished Young Scholars (Grant 50525207), the National Basic Research Program of China (Grant 2007CB936601), and the National Natural Science Foundation of China (10374092) for financial support.

(27) Meng, G. W.; Jung, Y. J.; Cao, A. Y.; Vajtai, R.; Ajayan, P. M. *Proc. Natl. Acad. Sci., U.S.A.* **2005**, *102*, 7074–7078.
(28) Inguanta, R.; Piazza, S.; Sunseri, C. *Electrochem. Commun.* **2008**, *10*, 506–509.

Note Added after ASAP Publication. After this paper was published ASAP on March 27, 2009, the authors were made aware of details of a published paper dealing with a similar topic. Reference 28 and the last paragraph of the Results and Discussion were added, and the updated version of this paper was published ASAP on May 14, 2009; minor revisions were made on May 18, 2009. Also, the Supporting Information file for the version of this paper published ASAP March 27, 2009 contained errors; the corrected version published ASAP March 31, 2009.

Supporting Information Available: Table S1 and Figures S1−S17 (PDF). This material is available free of charge via the Internet at http://pubs.acs.org.

CM803458B